ISSN 1674-1056
http://cpb.iphy.ac.cn
http://iopscience.iop.org/cpb
中国物理 B
Chinese Physics
中国物理
Chinese Physics B

Modification of short-range repulsive interactions in ReaxFF reactive force field for Fe-Ni-Al alloy

Huaqiang Chen(陈华强), Lin Lang(稂林), Shuaiyu Yi(易帅玉), Jinlong Du(杜进隆), Guangdong Liu(刘广东), Lixia Liu(刘丽霞), Yufei Wang(王宇飞), Yuehui Wang(王悦辉), Huiqiu Deng(邓辉球), and Engang Fu(付恩刚)
Citation: Chin. Phys. B, 2021, 30 (**8**): 086110. DOI: 10.1088/1674-1056/ac0901
Journal homepage: http://cpb.iphy.ac.cn; http://iopscience.iop.org/cpb

What follows is a list of articles you may be interested in

A novel two-dimensional SiO sheet with high-stability, strain tunable electronic structure, and excellent mechanical properties

Shijie Liu(刘世杰) and Hui Du(杜慧)
Chin. Phys. B, 2021, 30 (**7**): 076104. DOI: 10.1088/1674-1056/abf34d

Non-monotonic temperature evolution of nonlocal structure-dynamics correlation in CuZr glass-forming liquids

W J Jiang(江文杰) and M Z Li(李茂枝)
Chin. Phys. B, 2021, 30 (**7**): 076102. DOI: 10.1088/1674-1056/abf113

Heredity of clusters in the rapidly cooling processes of Al-doped $Zr_{50}Cu_{50}$ melts and its correlation with the glass-forming ability

Dadong Wen(文大东), Yonghe Deng(邓永和), Ming Gao(高明), and Zean Tian(田泽安)
Chin. Phys. B, 2021, 30 (**7**): 076101. DOI: 10.1088/1674-1056/abea93

Influence of temperature and alloying elements on the threshold displacement energies in concentrated Ni-Fe-Cr alloys

Shijun Zhao(赵仕俊)
Chin. Phys. B, 2021, 30 (**5**): 056111. DOI: 10.1088/1674-1056/abf10d

Mechanical property and deformation mechanism of gold nanowire with non-uniform distribution of twinned boundaries: A molecular dynamics simulation study

Qi-Xin Xiao(肖启鑫), Zhao-Yang Hou(侯兆阳), Chang Li(李昌), and Yuan Niu(牛媛)
Chin. Phys. B, 2021, 30 (**5**): 056101. DOI: 10.1088/1674-1056/abd162

SPECIAL TOPIC — Ion beam modification of materials and applications

Modification of short-range repulsive interactions in ReaxFF reactive force field for Fe–Ni–Al alloy*

Huaqiang Chen(陈华强)[1], Lin Lang(稂林)[2], Shuaiyu Yi(易帅玉)[2], Jinlong Du(杜进隆)[1], Guangdong Liu(刘广东)[2], Lixia Liu(刘丽霞)[2], Yufei Wang(王宇飞)[1], Yuehui Wang(王悦辉)[3], Huiqiu Deng(邓辉球)[2,†], and Engang Fu(付恩刚)[1,‡]

[1] *State Key Laboratory of Nuclear Physics and Technology, School of Physics, Peking University, Beijing* 100871, *China*
[2] *Department of Applied Physics, School of Physics and Electronics, Hunan University, Changsha* 410082, *China*
[3] *Department of Chemistry and Biology, University of Electronic Science and Technology of China Zhongshan Institute, Zhongshan* 528402, *China*

(Received 29 May 2021; revised manuscript received 4 June 2021; accepted manuscript online 8 June 2021)

The short-range repulsive interactions of any force field must be modified to be applicable for high energy atomic collisions because of extremely far from equilibrium state when used in molecular dynamics (MD) simulations. In this work, the short-range repulsive interaction of a reactive force field (ReaxFF), describing Fe–Ni–Al alloy system, is well modified by adding a tabulated function form based on Ziegler–Biersack–Littmark (ZBL) potential. The modified interaction covers three ranges, including short range, smooth range, and primordial range. The short range is totally predominated by ZBL potential. The primordial range means the interactions in this range is the as-is ReaxFF with no changes. The smooth range links the short-range ZBL and primordial-range ReaxFF potentials with a taper function. Both energies and forces are guaranteed to be continuous, and qualified to the consistent requirement in LAMMPS. This modified force field is applicable for simulations of energetic particle bombardments and reproducing point defects' booming and recombination effectively.

Keywords: molecular dynamics, force field modification, Fe–Ni–Al alloy, irradiation

PACS: 61.72.–y, 61.80.–x, 61.82.–d, 34.10.+x **DOI:** 10.1088/1674-1056/ac0901

1. Introduction

High energy (eV–keV) atomic collisions and kicking up atoms are common scenarios happened in sputtering, plasma etching, and nuclear irradiation.[1–4] To gain microscopic insights into these processes for experimental investigations, molecular dynamics (MD) simulations are widely used in recent decades. The basic of MD methodology is the Newton's laws of motion, and the core is the force field (or interatomic potential) that describes interactions among atoms consisting of the system under investigation. There have been a lot of studies aiming at the development of force field. The main tasks have been to make the potentials more accurate and efficient at describing the interactions. The ReaxFF potential developed by Van Duin *et al.*,[5] which has been implemented into the Large-scale Atomic/Molecular Massively Parallel Simulator (LAMMPS) molecular-dynamics package,[6] has so far found extensive applications to the diverse molecular and condensed materials, including hydrocarbons, carbon materials, silicon/silica structures, zeolites, metals, metal oxides, hydrides, biomolecules, plasma, and so on.[7] ReaxFF is a many-body potential composed of pair interaction, bond-angel interaction, and non-bonded interaction. ReaxFF centers the concept of bond order determined by interatomic distance between atom pairs. Unlike most other potentials which treat molecules as non-dissociable units, ReaxFF allows reactions between molecules based on their local chemical environment. The modeling of dissociations and reactivity is necessary since the atomic collisions caused by energetic atoms are known to trigger events of breaking and recombining bonds.

However, the repulsive force between pairs offered by ReaxFF itself is too weak to describe the strong repulsion in the short range typically below around 1 Å, because it is fitted for materials in the range of valence bond and Van der Waals interaction, which is typically around 2 Å to 10 Å. Hence, the ReaxFF potential must be connected to a repulsive potential to extend its applications involving high-energy atomic collisions.[8–12] Ziegler *et al.* have proven that the repulsive potential for any atom pair can be fairly accurately described by a universal potential in the form of a screened Coulomb term, usually called ZBL potential.[13] Up to now, many researches have successfully applied this to modify potentials for short range interaction, especially like Fe,[14,15] W,[16] and alloys[17] used in irradiation related studies.

The core of ReaxFF modification proposed here is to add one more tabulated pair potential based on ZBL poten-

*Project supported by the National Magnetic Confinement Fusion Energy Research Project (Grant Nos. 2019YFE03120003, 2018YFE0307100, and 2017YFE0302500) and the National Natural Science Foundation of China (Grant Nos. 11975034, 11921006, 12004010, and U20B2025).

†Corresponding author. E-mail: hqdeng@hnu.edu.cn
‡Corresponding author. E-mail: efu@pku.edu.cn

© 2021 Chinese Physical Society and IOP Publishing Ltd

tial to the basic ReaxFF, making the repulsive force and energy between colliding pair atoms correctly large enough to model close nuclear encounters in the short range. In order to shift atomic interaction gradually and smoothly from ZBL to ReaxFF as the pair atom distance goes large, a taper function is taken to spline and balance both potential equally in this transition range. Once coming into the valence range, we switch off the ZBL contribution. This modification is a common way for any ReaxFF and can be achieved in LAMMPS by hybrid pair style without modifying the ReaxFF parameters itself. The ReaxFF of Fe–Ni–Al alloys,[18] which may be used as nuclear materials, is taken here to go through the short-range modification and verified to be effectively simulating high energy atomic collisions.

2. Methods

2.1. Fitting the repulsive potential

The modified potential consists of the following two parts

$$E = E_{\text{tabulated}} + E_{\text{ReaxFF}}, \tag{1}$$

where E_{ReaxFF} is the as-is ReaxFF and $E_{\text{tabulated}}$ is the tabulated pair potential added to complement the repulsive pair interaction to a correctly level based on the ZBL potential. The modified interaction covers three ranges, including short range, transition range, and primordial range. The short range is totally predominated by ZBL. The primordial range means the interactions in this range is the as-is ReaxFF with no changes. The transition range shifts atomic interaction gradually and smoothly from ZBL to ReaxFF. Hence, the $E_{\text{tabulated}}$ can be expressed as

$$E_{\text{tabulated}} = \begin{cases} E_{\text{ZBL}} - E_{\text{ReaxFF}}, & r \in [0, R_1], \\ E_{\text{t}} - E_{\text{ReaxFF}}, & r \in [R_1, R_2], \\ 0, & r \in [R_2, \infty], \end{cases} \tag{2}$$

where r is the pair atom distance, E_{t} is the interaction energy in the transition range from R_1 to R_2. The ZBL potential E_{ZBL} for an atom pair i–j is given by

$$E_{\text{ZBL}} = \frac{1}{4\pi\varepsilon_0}\frac{Z_i Z_j}{r_{ij}}\phi\left(r_{ij}/a\right), \tag{3}$$

where $\phi\left(r_{ij}/a\right)$ is the screening function in the form of

$$\begin{aligned}\phi(x) = {} & 0.18175\,\mathrm{e}^{-3.19980x} + 0.50986\,\mathrm{e}^{-0.94229x} \\ & + 0.28022\,\mathrm{e}^{-0.40290x} + 0.02817\,\mathrm{e}^{-0.20162x}\end{aligned} \tag{4}$$

and a is the screening length given by

$$a = \frac{0.46850}{Z_i^{0.23} + Z_j^{0.23}}. \tag{5}$$

For pair interaction, force is the negative gradient of energy over the pair distance of r values. Thus, the force of the tabulated potential is

$$E_{\text{tabulated}} = \begin{cases} E_{\text{ZBL}} - E_{\text{ReaxFF}}, & r \in [0, R_1], \\ E_{\text{t}} - E_{\text{ReaxFF}}, & r \in [R_1, R_2], \\ 0, & r \in [R_2, \infty], \end{cases} \tag{6}$$

where F_{ZBL} and F_{ReaxFF} are the pair forces offered by ZBL and ReaxFF potential, respectively. F_{t} is the force acting on the transition range. In order to shift atomic interaction gradually and smoothly from ZBL to ReaxFF as the pair atom distance goes large, a taper function is taken to balance both potentials equally in this transition range as the following expression:

$$\begin{aligned} F_{\text{t}} = {} & \text{Taper}(r) \cdot \left[F_{\text{ZBL}} - F_{\text{ReaxFF}}\right] + F_{\text{ReaxFF}}, \\ & r \in [R_1, R_2], \end{aligned} \tag{7}$$

where

$$\begin{aligned}\text{Taper}(r) = {} & \left[1 - 35\left(\frac{r-R_1}{R_2-R_1}\right)^4 + 84\left(\frac{r-R_1}{R_2-R_1}\right)^5\right. \\ & \left. - 70\left(\frac{r-R_1}{R_2-R_1}\right)^6 + 20\left(\frac{r-R_1}{R_2-R_1}\right)^7\right]. \end{aligned} \tag{8}$$

Finally, the tabulated pair potential can be obtained by integrating the tabulated force on distance, *i.e.*,

$$E_{\text{tabulated}} = -\int_{R_2}^{0} F_{\text{tabulted}}\mathrm{d}r. \tag{9}$$

2.2. Simulation parameters

All these molecular dynamics simulations mentioned in this work are conducted in LAMMPS. The pair style of hybrid/overlay is implanted to superpose the tabulated pair potential to the ReaxFF. The control setting of the ReaxFF pair style is specified as NULL, in which case default settings are used. The global cutoff distance is set to 10 Å. All atoms are assigned zero charge initially and charge equilibration is executed every step by using electronegativity equalization method (EEM)[19] to handle the electrostatic interactions among atoms every step until a precision of $10^{-3}e$ has reached, where e is the elementary electric charge. The modification procedure is conducted by home-made shell and MATLAB scripts. The tabulated forces and tabulated energies are consistent (*i.e.*, $\mathrm{d}E/\mathrm{d}r = -F$) over the entire range of r values. The distance interval is 0.001 Å. Both energies and forces are guaranteed to be continuous, and qualified to the consistent requirement of 10^{-6} eV/Å in LAMMPS with no warnings.

The atomic model used to verify the modification of the short-range repulsive interaction of Fe–Ni–Al system is a box of body-centered-cubic (BCC) Fe with an $L2_1$-Ni_2FeAl precipitate[20] in its center as the square indicates in Fig. 1(a). The contacting interface of $L2_1$-Ni_2FeAl with BCC Fe matrix consists of Fe and Al atoms orderly as the blue square lines in Fig. 1(b). The unit cell of $L2_1$-Ni_2FeAl is also provided in Fig. 1(c). The size and atom number of this model are listed in Table 1.

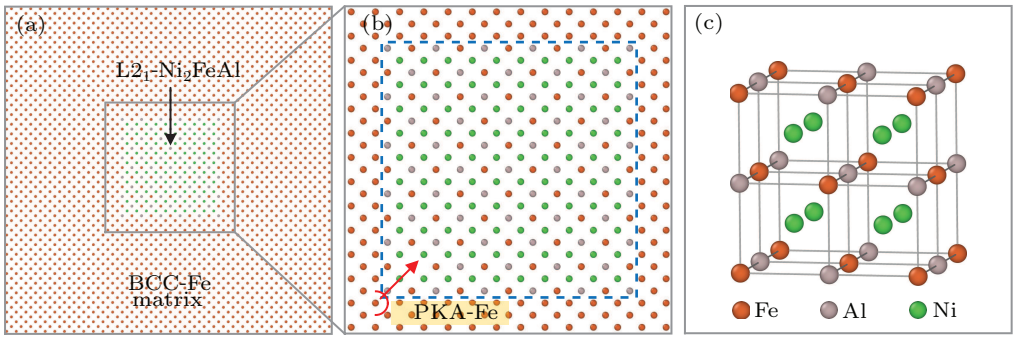


Fig. 1. Atomic structure of (a) overall view and (b) magnified view of BCC-Fe matrix containing a precipitate composed of (c) $L2_1$-Ni_2FeAl. Fe, Al, and Ni atoms are colored with orange, grey, and green, respectively.

Table 1. The size and atom number of BCC-Fe with an $L2_1$-Ni_2FeAl.

Structure	Size (Å)	Atoms
BCC-Fe	$96.64 \times 96.64 \times 96.64$	76276
$L2_1$-Ni_2FeAl	$28.60 \times 28.60 \times 28.60$	2332

The simulation system is firstly relaxed within the NVT ensemble (constant number of atoms, volume, and temperature) at 300 K for 10 ps with a time step of 0.25 fs. In high energy collision stage, NVE ensemble (constant number of atoms, volume, and total energy) is employed. An Fe atom below the left-corner of $L2_1$-Ni_2FeAl precipitate is selected to be the primary knock-on atom (PKA) with kinetic energy of 10 keV to strike high energy cascade collisions, launching from its lattice site where it initially locates in and heading towards the precipitate along [111] direction as shown in Fig. 1(b). During this stage, atoms within a shell of approximately 0.3 nm from the outer margin of the simulation box are applying with the velocity rescaling method every 10 steps to keep temperature at 300 K. The time step varies from 1×10^{-3} fs to 2.5×10^{-1} fs depending on the atomic velocities to make sure that the maximum distance of any atom is within 0.02 Å in every step. Periodic boundary conditions are applied in all three Cartesian directions throughout the simulation. All snapshots are visualized by the Open Visualization Tool (OVITO).[21] The Wigner–Seitz method was used to identify vacancies, interstitials, and anti-sites.[22]

3. Results and discussion

In order to have a direct-viewing impression on how weak the interatomic repulsive force offered by ReaxFF is, a collision cascade simulation is conducted with ReaxFF only as mentioned in Fig. 1(b) early and snapshotted in Fig. 2. At $t = 0.43$ fs, the PKA is just launched off a little bit from its lattice site as figure 2(a) shows. At $t = 5.86$ fs, the PKA has passed four atoms through its trajectory along [111] without any visually evident collision event in Fig. 2(b). When time goes to $t = 18.40$ fs, no collision cascade has happened yet and only two recoil atoms are observed slightly off their lattice sites as figures 2(c) and 2(d) show. As mentioned early in methods, maximum distance of any atom is restricted within 0.02 Å in every step by means of variable timestep in simulation. Generally, the interatomic repulsive force increases dramatically to infinity due to the internuclear electrostatic interaction when atom pair distance comes to a short range. Hence, it has enough interactions for PKA to collide and repel atoms off its trajectory. However, only poor kinetic energies have transferred to these two recoil atoms, *i.e.*, 6.0 eV for Ni atom and 4.4 eV for Al. All these hint that the ReaxFF can only provide poor repulsive force when pairs close in short range, and must be modified to increase the repulsive interaction to describe the collision scenarios correctly.

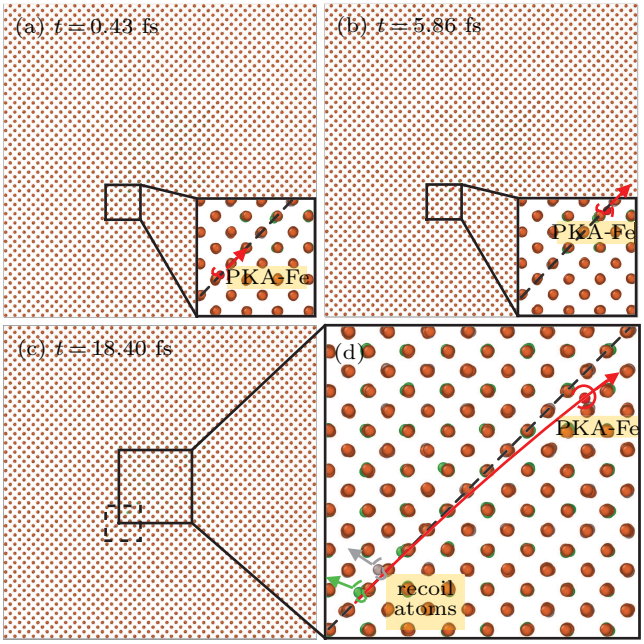


Fig. 2. The snapshots of weak collision cascade happened in BCC-Fe matrix containing an $L2_1$-Ni_2FeAl precipitate conducted only with ReaxFF at (a) $t = 0.43$ fs, (b) $t = 5.86$ fs, (c) $t = 18.40$ fs, and (d) a typical weak collision event happened at the moment. The PKA atom is circled and colored with red and arrows indicate velocity directions. The black dashed line refers the [111] direction. The solid red line in panel (d) records the PKA trajectory, and the recoiled Al and Ni atoms are also circle with grey and green, respectively. The enlarged area in panels (a) and (b) are the same, and also indicated in panel (c) by a black dashed square for reference.

The repulsive force offered by ReaxFF is so weak only at the level of 10^3 eV/Å as the green dashed lines show in

Fig. 3(a) for instance. In order to reproduce the repelling process in high energy atomic collision simulations correctly, it is necessary to complement the weak repulsive pair interaction to a correctly level based on the ZBL potential. The ZBL potential must be smoothly connected to the given near-equilibrium potential as the blue solid curves show in Fig. 3(a). This is achieved by a taper function as mentioned early in Eq. (8), equally shifting from one to another one as distance increases within the transition range. The terminal values of transition region (R_1, R_2) for Al–Al is (1.7, 2.3), while (1.8, 2.4) is taken for the rest five kinds of atomic pairs including Fe–Fe, Fe–Al, Fe–Ni, Al–Ni, and Ni–Ni. All these modified ranges are within the first neighboring distances of equilibrium states, making sure that these modifications have no effect to the equilibrium states of materials. The interatomic energy curves go down dramatically around 2.4 Å for Figs. 3(a) and 3(c), and 2.1 Å for Figs. 3(b) and 3(d) as a result of the energies come to zero here in the logarithmic coordinates. The zero points of interatomic potential energy curves, where the values are zero, look like retarded towards left a little bit when compared to the force curve, because potential energy of the tabulated force field is calculated by numerical integration of the force.

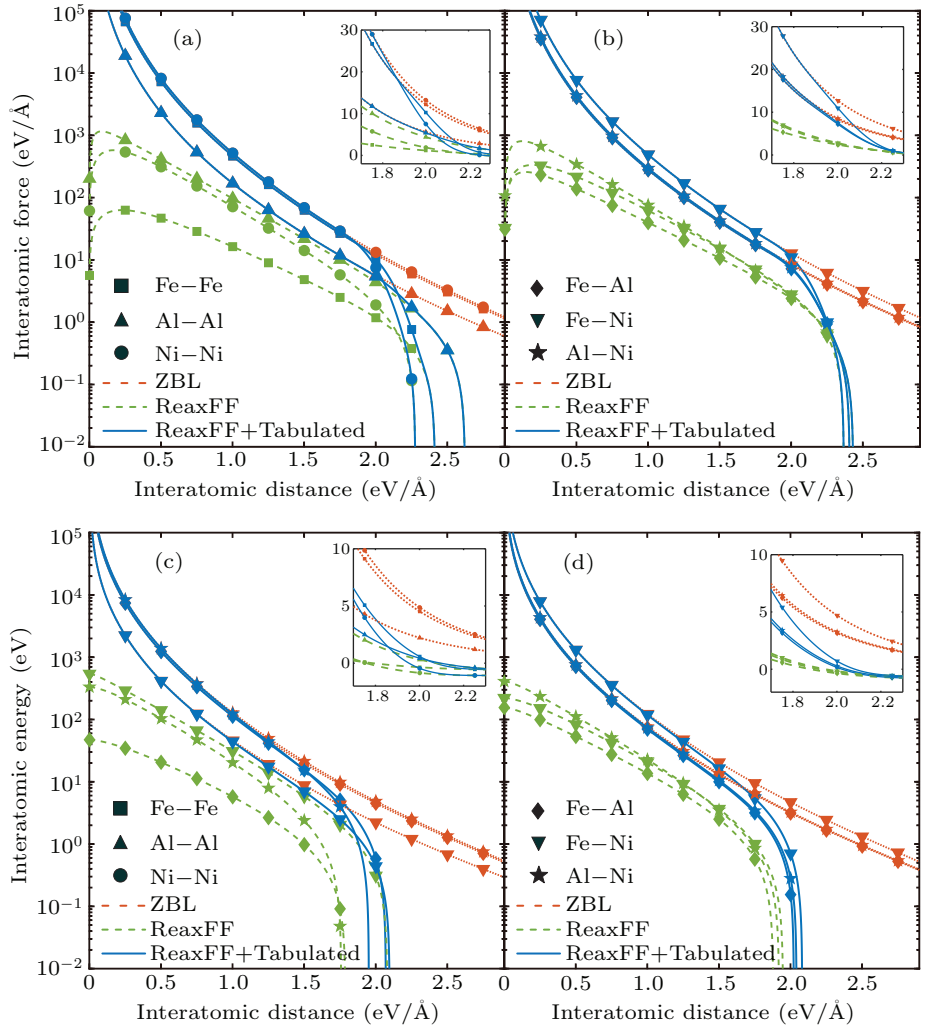


Fig. 3. The comparison of homogenous atom pair interactions in (a) interatomic force and (b) interatomic energy including Fe–Fe (squares), Al–Al (upward triangles), and Ni–Ni (circles). The comparison of heterogenous atom pair interactions in (c) interatomic force and (d) interatomic energy including Fe–Al (diamonds), Fe–Ni (downward triangles), and Al–Ni (pentagrams). The interatomic force and energy of the short-range interactions predicted by the ZBL potential (orange dotted line), the ReaxFF (green dashed line), and the ReaxFF with the additional tabulated potential (blue solid line) are self-explained as these legends show at the left-lower corners. The insets at the right-upper corners show more spline connection details of the interaction curves in the range of 1.7 Å to 2.3 Å.

The taper function (see Eq. (8)) behaves superior spline performance than the usually used the fourth order exponential polynomial (FOEP) (see Eq. (10)) in connecting potential curves of ZBL and basic potential which describes of the equilibrium properties. Because the FOEP only takes the forces

$$E(r) = \exp\left(B_0 + B_1 r + B_2 r^2 + B_3 r^3\right), \quad r \in [R_1, R_2], \tag{10}$$

$$\begin{bmatrix} 1 & R_1 & R_1^2 & R_1^3 \\ 1 & R_2 & R_2^2 & R_2^3 \\ 0 & 1 & 2R_1 & 3R_1^2 \\ 0 & 1 & 2R_2 & 3R_2^2 \end{bmatrix} \begin{bmatrix} B_0 \\ B_1 \\ B_2 \\ B_3 \end{bmatrix} = \begin{bmatrix} \ln E_1 \\ \ln E_2 \\ -F_1/E_1 \\ -F_2/E_2 \end{bmatrix}, \tag{11}$$

(F_1 and F_2) and energies (E_1 and E_2) at the two connecting points (R_1 and R_2) into account in which parameters (includ-

ing B_0, B_1, B_2, B_3) are determined by (Eq. (11)), so usually LAMMPS will warn that some force values in table are inconsistent with $-\mathrm{d}E/\mathrm{d}r$ and reminder that values should only be flagged at inflection points. More, the FOEP is always positive, and cannot be employed in the negative range of potential. While taper function acts as an adjuster which considers the both two connected potential in this connecting range equally, making the transition curve smooth enough and avoiding the warning by LAMMPS. For a more general illustration, let us consider two curves ($A(r)$ and $B(r)$) needed to be connected. The connection function based on Taper function, like Eq. (7), is expressed by

$$C(r) = \mathrm{Taper}(r) \cdot [A(r) - B(r)] + B(r), \quad r \in [R_1, R_2]. \quad (12)$$

As visualized in Fig. 4, the values of Taper function gradually shift from 1 to 0 as the interatomic distances r increase from R_1 to R_2. Easily, we will see that the connection function $C(r) = A(r)|_{r=R_1}$ and $C(r) = B(r)|_{r=R_2}$ at the two terminal points. And during the connection range $[R_1, R_2]$, $C(r)$ gradually shifts from $A(r)$ to $B(r)$. The maximum shift is happened in the mid-point $(R_1 + R_2)/2$ as the first-order derivative curve presents. One more understanding about the Taper function and its first-order derivative is that these two function curves are constant with variables R_1 and R_2. This specialty origins the normalization in function definition with $(r - R_1)/(R_2 - R_1)$ in Eq. (8), making the Taper function to be universal.

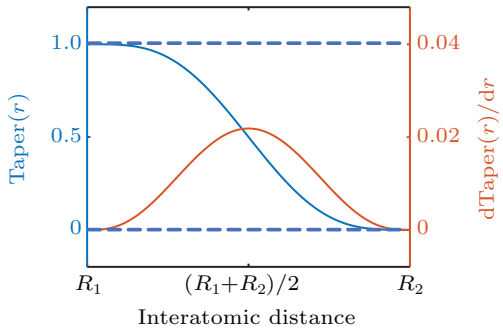


Fig. 4. The curves of Taper function (blue) and its first-order derivative (orange).

The reliability of the modification of ReaxFF force field used in this paper is evaluated, and some basic properties of Fe, Al, and Ni have been calculated by LAMMPS and summarized in Table 2. As we can see, the modifications in short-range do not influence the basic properties near equilibrium, including lattice constants, cohesive energies, defect formation energies of vacancy, and dumbbells ([100], [110], [111]). This is easy to understand because the modification range is shorter enough than the first neighboring distance. However, we also noticed that the as-is ReaxFF failed at predicting the dumbbell formation energies in BCC-Fe, in which dumbbell pair of Fe–Fe is more stable along [111] than [110]. In fact, [110] should be the stable one in magnetic BCC metals. The tabulated potential added here cannot correct this. Although refitting of the as-is ReaxFF may be needed in the future, the modification method in short range we stated here works effectively.

Table 2. The lattice constants, cohesive energies, defect formation energies including vacancy and dumbbells ([100], [110], [111]) evaluated by the ReaxFF force field, hybridizing ReaxFF with tabulated pair potential (denoted as ReaxFF+Tab), and previous approved references for pure condensed ground-state phase in Fe–Ni–Al system.

Parameters	Potential	Fe (BCC)	Al (FCC)	Ni (FCC)
Lattice constant (Å)	ReaxFF	2.8406	4.0402	3.5244
	ReaxFF+Tab	2.8406	4.0402	3.5244
	Ref.	2.8333[23]	4.0496[24]	3.5240[24]
Cohesive energy (eV)	ReaxFF	–4.39	–3.40	–4.42
	ReaxFF+Tab	–4.39	–3.40	–4.42
	Ref.	–4.28[25]	–3.39[25]	–4.44[25]
$E_{\mathrm{v}}^{\mathrm{f}}$ (eV)	ReaxFF	2.75	0.89	1.67
	ReaxFF+Tab	2.75	0.89	1.67
	Ref.	1.71[26]	0.67[27]	1.57[28]
$E_{\mathrm{d100}}^{\mathrm{f}}$ (eV)	ReaxFF	3.69	2.78	4.11
	ReaxFF+Tab	3.69	2.78	4.11
	Ref.	4.34[26]	3.01[27]	3.95[28]
$E_{\mathrm{d110}}^{\mathrm{f}}$ (eV)	ReaxFF	3.44	2.98	4.43
	ReaxFF+Tab	3.44	2.98	4.43
	Ref.	3.52[26]	3.05[27]	4.28[28]
$E_{\mathrm{d111}}^{\mathrm{f}}$ (eV)	ReaxFF	3.26	3.23	4.65
	ReaxFF+Tab	3.26	3.23	4.65
	Ref.	4.04[26]	3.80[27]	4.21[28]

To validate the modification does affect in short range, a same collision cascade simulation mentioned early in Fig. 1(b) is conducted by using ReaxFF hybridizing with the tabulated pair potential and snapshotted in Fig. 5. At $t = 0.00$ ps, the PKA is just launching off from its lattice site as figure 5(a) shows. At $t = 0.04$ ps, the PKA has ignited some visually evident collision events along its trajectory in Fig. 5(b), while atoms far away from collision zones are unaffected and remain staying in their lattice sites as the depict presents. As time goes by, displacement cascades arise out caused by much more kicked-out lattice atoms whose energies are transferred from PKA, corresponding to the ballistic stage indicated in Fig. 5(g). When time comes to $t = 0.10$ ps, many atoms are observed obviously off their lattice sites as figure 5(c) shows. The atoms gradually collide each other violently and reach to thermal spike stage furthest at $t = 0.20$ ps in which the majority of atoms are temporarily in motion in Fig. 5(d). After that, the high kinetic energies possessed by cascade atoms will be shared between neighboring atoms and cool down as lattice vibrations or what we called heat. The damaged cascade zones are going to recover and point defects recombine as shown in Fig. 5(e). After 4.70 ps from very beginning, the cascade caused an energetic PKA nearly comes to an end reaching to

a new equilibrium with few point defects remained which are indicated by blue arrows in depict in Fig. 5(f).

All these testify that the modified ReaxFF can provide enough repulsive force when pairs close in short range, and describe the collision scenarios correctly. Fe–Ni–Al alloys are known to offer enhanced corrosion resistance under high temperature and oxidizing environment. With the modified potential, a way is paved to analyze microstructures' evolutions of Fe–Ni–Al alloys used in complex extreme environments under irradiation, especially cladding materials in nuclear reactors.

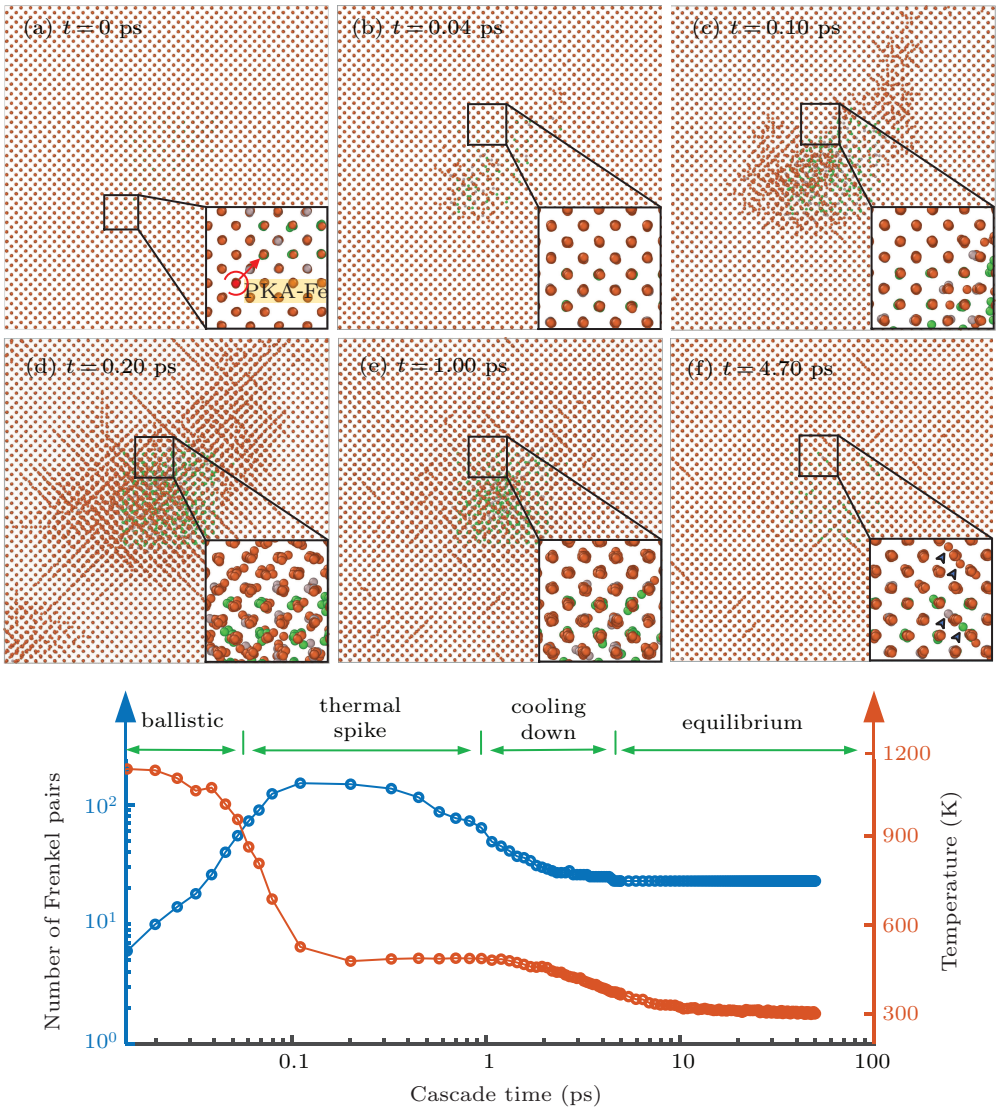


Fig. 5. The snapshots of collision cascade happened in BCC-Fe matrix containing an $L2_1$-Ni_2FeAl precipitate conducted with short range modified ReaxFF at (a) $t = 0.00$ ps, (b) $t = 0.04$ ps, (c) $t = 0.10$ ps, (d) $t = 0.20$ ps, (e) $t = 1.00$ ps, and (f) $t = 4.70$ ps in the case of $E_{PKA} = 10$ keV. The PKA atom is circled and colored with red and arrows indicating velocity directions. The enlarged area in panels (b)–(f) are the same. Some interstitial atoms remain after thermal spike as blue arrows indicate in panel (f). (g) The number of Frenkel pairs (blue curve) and temperature at the core of cascade (orange curve) as a function of simulation time during cascade simulation.

4. Conclusion and perspectives

The existed ReaxFF reactive force field for Fe–Ni–Al alloy have been modified in short-range repulsive interaction based on ZBL potential by adding a tabulated pair potential. The smooth range links the short-range ZBL and primordial-range ReaxFF with a taper function. Both energies and forces are guaranteed to be continuous, and qualified to the consistent requirement of 10^{-6} eV/Å in LAMMPS. The modified force field is applicable and examined for simulations of energetic particle bombardments in Fe–Al–Ni alloy system, and does not affect the properties in equilibrium. This modification is a common way for any ReaxFF and can be achieved in LAMMPS by hybrid pair style without modifying the ReaxFF parameters itself.

Acknowledgments

One of the authors (E G Fu) appreciates the Ion Beam Materials Lab at Peking University and the Instrumental Analysis Fund of Peking University. The authors thank the High-performance Computing Platform of Peking University for the support of calculations.

References

[1] Lin Y, Yang T, Lang L, Shan C, Deng H, Hu W and Gao F 2020 *Acta Materialia* **196** 133

[2] Nastasi M A, Mayer J W and Hirvonen J K 2004 *Ion-solid interactions: fundamentals and applications* (Cambridge; New York: Cambridge University Press) pp. 218–221

[3] Beyerlein I J, Demkowicz M J, Misra A and Uberuaga B P 2015 *Prog. Mater. Sci.* **74** 125

[4] Fu E G, Caro M, Zepeda-Ruiz L A, Wang Y Q, Baldwin K, Bringa E, Nastasi M and Caro A 2012 *Appl. Phys. Lett.* **101** 191607

[5] Chenoweth K, van Duin A C T and Goddard W A 2008 *J. Phys. Chem. A* **112** 1040

[6] Plimpton S 1995 *J. Comput. Phys.* **117** 1

[7] Senftle T P, Hong S, Islam M M, Kylasa S B, Zheng Y, Shin Y K, Junkermeier C, Engel-Herbert R, Janik M J, Aktulga H M, Verstraelen T, Grama A and van Duin A C T 2016 *npj Comput. Mater.* **2** 15011

[8] Smith R, Jolley K, Latham C, Heggie M, van Duin A, van Duin D and Wu H Z 2017 *Nucl. Instrum. Methods Phys. Res. Sect. B* **393** 49

[9] Anders C and Urbassek H M 2013 *Nucl. Instrum. Method B* **303** 200

[10] Kanski M, Maciazek D, Postawa Z, Ashraf C M, van Duin A C T and Garrison B J 2018 *J. Phys. Chem. Lett.* **9** 359

[11] Byggmastar J, Granberg F and Nordlund K 2018 *J. Nucl. Mater.* **508** 530

[12] Liu L C, Liu Y, Zybin S V, Sun H and Goddard W A 2011 *J. Phys. Chem. A* **115** 11016

[13] Ziegler J F, Ziegler M D and Biersack J P 2010 *Nucl. Instrum. Methods Phys. Res. Sect. B* **268** 1818

[14] Ackland G J, Bacon D J, Calder A F and Harry T 1997 *Philos. Mag. A* **75** 713

[15] Malerba L, Marinica M C, Anento N, Bjorkas C, Nguyen H, Domain C, Djurabekova F, Olsson P, Nordlund K, Serra A, Terentyev D, Willaime F and Becquart C S 2010 *J. Nucl. Mater.* **406** 19

[16] Chen Y C, Li Y H, Gao N, Zhou H B, Hu W Y, Lu G H, Gao F and Deng H Q 2018 *J. Nucl. Mater.* **502** 141

[17] Bonny G, Castin N, Bullens J, Bakaev A, Klaver T C P and Terentyev D 2013 *J. Phys.: Condens. Matter* **25** 31

[18] Shin Y K, Kwak H, Zou C Y, Vasenkov A V and van Duin A C T 2012 *J. Phys. Chem. A* **116** 12163

[19] Mortier W G and Shankar, S 1986 *J. Am. Chem. Soc.* **108** 4315

[20] Baik S I, Wang S Y, Liaw P K and Dunand D C 2018 *Acta Materialia* **157** 142

[21] Stukowski A 2010 *Model. Simul. Mater. Sci.* **18** 015012

[22] Stukowski A, Bulatov V V and Arsenlis A 2012 *Model. Simul. Mater. Sci.* **20** 8

[23] Haas P, Tran F and Blaha P 2009 *Phys. Rev. B* **79** 085104

[24] Tran R, Xu Z H, Radhakrishnan B, Winston D, Sun W H, Persson K A and Ong S P 2016 *Sci. Data* **3** 160080

[25] Kittel C and McEuen P 2018 *Introduction to solid state physics* (Hoboken: John Wiley & Sons) p. 20

[26] Mendelev M I, Han S W, Son W J, Ackland G J and Srolovitz D J 2007 *Phys. Rev. B* **76** 214105

[27] Pascuet M I and Fernandez J R 2015 *J. Nucl. Mater.* **467** 229

[28] Pun G P P and Mishin Y 2009 *Philos. Mag.* **89** 3245